ART & TECHNOLOGY PUBLISHING PTE. LTD.

Information Engineering and Applied Computing

2023 Volume 2, Issue 1

ISSN: 2630-4619

Development of Low-Cost 3D Printing Bi-Axial Pressure Sensor

Heonsoo Choi, Joonseong Yeo, Jihun Seong, Hyunjin Choi*

Department of Human Intelligence Robot Engineering, Sangmyung University, Cheonan, Republic of Korea

***Corresponding author:** Hyunjin Choi, hyunjin@smu.ac.kr

Abstract

As various mobile robots and manipulator robots have been commercialized, robots that can be used by individuals in their daily lives have begun to appear. With the development of robots that support daily life, the interaction between robots and humans is becoming more important. Manipulator robots that support daily life must perform tasks such as pressing buttons or picking up objects safely. In many cases, this requires expensive multi-axis force/torque sensors to measure the interaction. In this study, we introduce a low-cost two-axis pressure sensor that can be applied to manipulators for education or research. The proposed system used three force-sensitive resistor (FSR) sensors and the structure was fabricated by 3D printing. An experimental device using a load cell was constructed to measure the biaxial pressure. The manufactured prototype was able to distinguish the +-x-axis and the +-y-axis pressures.

Keywords

Pressure sensor
2-axis force sensor
3D printer

1. Introduction

The range of robot applications has expanded not only in industrial applications but also into human daily life. Cooking robots and serving robots have emerged in restaurants, and domestic assistance robots capable of tasks such as dishwashing, cleaning, and laundry are being developed for household use. These robots primarily carry out their assigned tasks through manipulations. However, manipulators operating in spaces alongside humans can potentially cause injuries and damage objects made of materials such as glass and plastic. Therefore, precise measurement of interaction forces and robust force control are required. High-cost commercial multi-axis force/torque sensors are commonly used for precise interaction force measurement, which can pose difficulties for various manipulator-related research.

Large manipulators, such as factory robots,

often require measurement of significant forces, and research has been conducted to create multi-axis force sensors using strain gauges [1-5]. Recently, research has progressed on the development of multi-axis force sensors that can be easily fabricated using three-dimensional (3D) printers. Hendrich *et al.* presented a six-axis torque-moment sensor that can be fabricated through 3D printing [6]. They combined spiral spring and cantilever structures and used acrylonitrile butadiene styrene (ABS) and polylactic acid (PLA) filaments as 3D printing materials. A photo-interrupter is used to measure the change in resistance which is up to about 11 N of forces. While it offers the advantage of measuring forces and moments in all six axes, it has the disadvantage of being relatively large, including the sensor itself. Strain gauge-type sensors have the advantage of precisely measuring large forces but are typically used in conjunction with rigid and heavy structures. Additionally, they can become bulkier due to the addition of amplifiers, Wheatstone bridge circuits, and other components. Kim *et al.* presented a three-axis force sensor that can be fabricated using 3D printing [7]. It is constructed with monolithic beams featuring sensing parts printed with carbon nanotubes (CNT) / thermoplastic polyurethane (TPU) on the surface. It offers the advantage of customizable design and material modification to meet user requirements, with a measurement range of up to 4 N. While multi-axis sensors fabricated using 3D printing have the advantage of a straightforward manufacturing process, they have the disadvantage of either requiring additional expensive sensors or having a limited force measurement range [8].

Recently, soft sensors made of gentle materials have also been developed for comfortable and safe interaction between humans and robots [9-16]. However, soft sensors often have a smaller force measurement range than rigid sensors, and their manufacturing processes can be complex, requiring costly equipment. Additionally, they tend to have low durability and exhibit significant hysteresis due to material characteristics.

Given the increasing need for affordable and safe multi-axis force sensors that can be used with various manipulators, this research proposes a bi-axial pressure sensor that can be easily fabricated using 3D printing and low-cost sensors. The design and fabrication process of the bi-axial pressure sensor is introduced, and the force measurement performance of the completed sensor is experimented with. In addition, simple experiments are conducted to show that the proposed sensor can be applied to robotic grippers or wearable devices.

2. Bi-axial pressure sensor design and fabrication

2.1. Low-cost pressure sensor

In this study, the force-sensitive resistor (FSR) RA12P model from MarvelDex was primarily utilized without using strain gauges commonly used for multi-axis force sensors. This model offers the advantage of ease of use, as it undergoes changes in resistance due to pressure without the need for additional amplifiers of Wheatstone bridge circuits, and is available at a relatively affordable price of less than 10,000 KRW.

2.2. Principles and structure of bi-axial pressure measurement

The FSR-RA12P has dimensions of 14.15 mm in length, 12 mm in width, 1.55 mm in thickness, a sensing area with a diameter of 4.8 mm, and a maximum force measurement range of 4–5 kg. The proposed bi-axial pressure sensor in this study used three FSR-RA12P sensors. The left image in **Figure 1** is an exploded view of the bi-axial pressure sensor and the right image in **Figure 1** shows a cross-sectional view of the bi-axial pressure sensor. In the image, the red part represents the head, the purple part represents the pillar, and the teal part represents the body. These three parts are used to create the bi-axial pressure sensor. The three FSR sensors are embedded in the inner wall of the body. To

ensure contact with the inner wall of the body, three radial protrusions were designed on the head. The left image in **Figure 2** shows a view from below the head. The protrusions on the head make contact with the FSR on the body, allowing the head to apply pressure to the FSR according to the force in each axial direction. Holes are created at the bottom of the body for the wiring of each FSR sensor. The proposed bi-axial pressure sensor uses the characteristics of a cantilever beam where the bottom is fixed, and the head makes contact with the FSR due to the deformation of the pillar, transmitting external force. To ensure a strong fixation at the bottom, the pillar and body are initially designed in a clamping shape at the bottom and secured with 8 bolts and nuts. The pillar and head are also secured in the same way with 6 bolts and nuts.

While multi-axis force sensors using strain gauge methods typically require four sensors in the +x, -x, +y, and -y directions, in this study, three FSR sensors were arranged at 120° intervals to measure 2-axis forces with a reduced number of sensors [17].

2.3. Prototype fabrication using 3D Printing

When force is applied to the head of the sensor, the head transmits the force to the pillar, and the pillar deforms similarly to a cantilever beam under external forces. The deformed pillar then causes the head to exert pressure on the FSR sensor. To ensure that the reactionary force is effectively transmitted between the head and body, the body requires sufficient strength. To satisfy this condition, the body was 3D printed using PLA filaments, which have high strength, can withstand large forces without breaking or cracking, and have a low deformation rate.

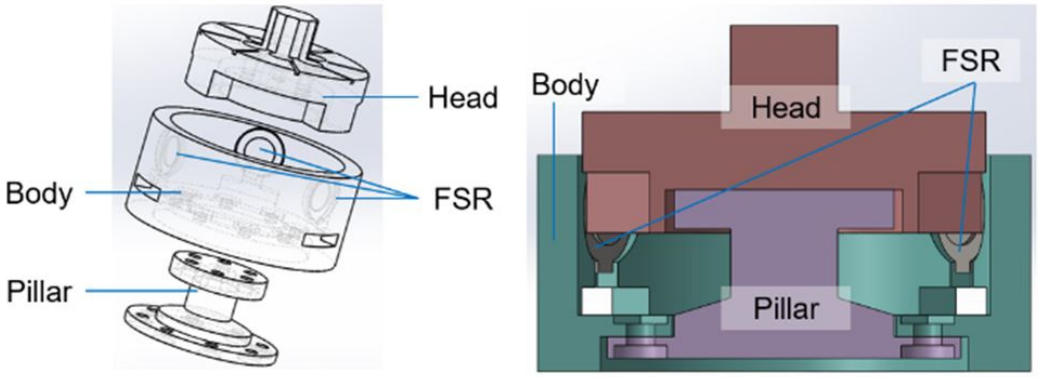

Figure 1. Exploded view (left) and sectional view (right) of the proposed bi-axial pressure sensor

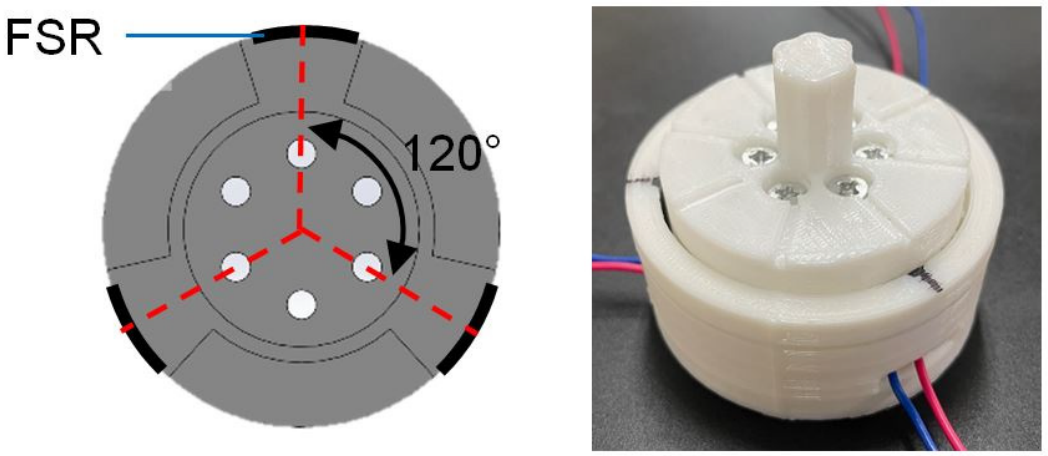

Figure 2. (Left) bottom view of the head, and (right) the completed bi-axial pressure sensor

The head is positioned at the top of the bi-axial pressure sensor and is responsible for receiving external force from the protrusions and transmitting them to the FSR. To ensure that the FSR sensor is slightly compressed by the head without applying additional external forces after assembly, the head was designed slightly larger and 3D printed using TPU material, which is deformable and has a restoring force. The direction of the external force applied to the head determines whether the FSR receives a stronger or weaker pressure compared to its initial state. The output values of the three sensors can be used to determine the magnitude and direction of the external force.

The right image in **Figure 2** shows the assembly of 3D-printed components and FSR sensors, completing the fabrication of the bi-axial pressure sensor. The finished bi-axial pressure sensor has cylindrical dimensions with a diameter of 55 mm and a height of 40 mm. A hatched pattern was added to the top of the head to facilitate the confirmation of the FSRs' position from above.

3. Bi-axial force measurement experiment

3.1. Experimental setup and environment

Figure 3 illustrates the configuration of the measurement setup for measuring the direction and magnitude of force along each axis using the bi-axial pressure sensor. To accurately measure the force, a measurement setup using CAS's MNC-50L load cell was created. The sensing area of the load cell is positioned horizontally, corresponding to the protrusion on the head of the bi-axial pressure sensor. When a force is applied by pushing the load cell, it maintains a horizontal position and moves along a rail to transmit the force. The force applied to the load cell is then transmitted to the protrusions on the bi-axial pressure sensor through a force transmission auxiliary mechanism. To ensure accurate measurements, the bi-axial pressure sensor is fixed in place on the test bed to prevent it from moving When measuring the force in the +x, -x, +y, and -y directions of the bi-axial pressure sensor, the sensor is rotated, and adjusted according to the axis set in **Figure 3**. The three FSRs are defined as FSR0, FSR1, and FSR2, and their colors correspond to those shown in the graphs in the experimental results. The current state represents the measurement in the +x direction.

The three FSR sensors included in the fabricated force sensor, along with the load cell, are measured using the Analog Input of National Instruments' myRIO, as shown in **Figure 4**. Because the load cell outputs very low voltage values, the signals are amplified before measurement using amplifiers. Measurements were taken with a sampling frequency of 100 Hz on myRIO. The measured data is transferred to the HOST PC via transmission control protocol/ internet protocol (TCP/IP) communication for data storage and visualization graph plotting.

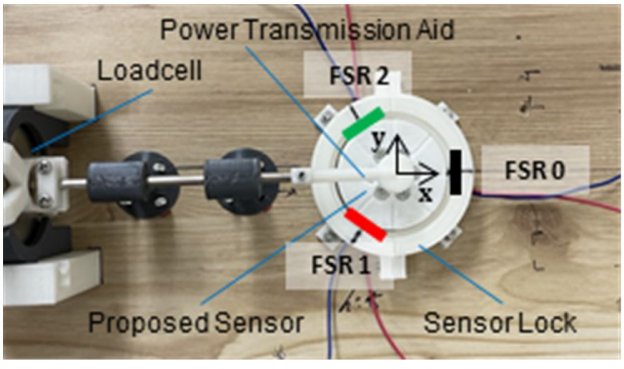

Figure 3. Experimental setup using the load cell, the proposed sensor, and the axis configuration

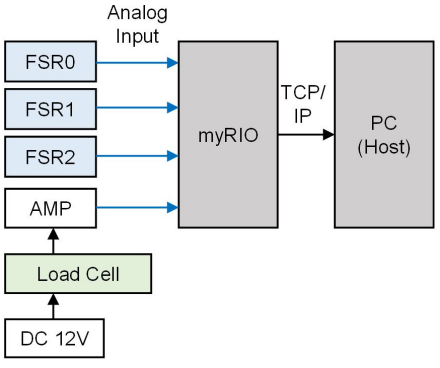

Figure 4. System configuration diagram for the experiment

3.2. Experimental results

When considering the FSR sensor measurement values as S^r_0, S^r_1, and S^r_2, the sensor values used for force measurement are calculated as follows, excluding the initial values.

$$FSR_i(k)=S^r_i(k)-b_i \quad (1)$$

Here, i={0,1,2}, and b_i is defined as the average of S^r_i values during the initial state where no force is applied to the bi-axial pressure sensor module for the first 4 seconds.

3.2.1. X-axis pressure experiment

In accordance with **Figure 5**, forces ranging from 0 to 2 kg were applied in both the +x and -x directions, and the sensor values were measured. The experiment involved a total of three cycles, each cycle starting from the unloading state, reaching the peak leading point (2 kg), waiting for about 5 seconds, returning to the unloading state, and waiting for 5 seconds.

Figure 6 shows the measured values of the three FSR sensors and the load cell measurement for the +x direction of force. A constant load cell measurement indicates a consistent force, and the experimental setup was designed to apply force only along the specified axis. For the +x direction of force, FSR0 experiences pressure, and its measurement value increases, while FSR1 and FSR2 move away from the head in the initial state, causing their measurement values to decrease. The experimental results align with these assumptions, with FSR0 having positive values and the other sensors having negative values.

Figure 7 presents the experimental results for the -x direction of force using the same method. Since FSR1 and FSR2 are positioned at the same angle as the x-axis, their measurement values should ideally be

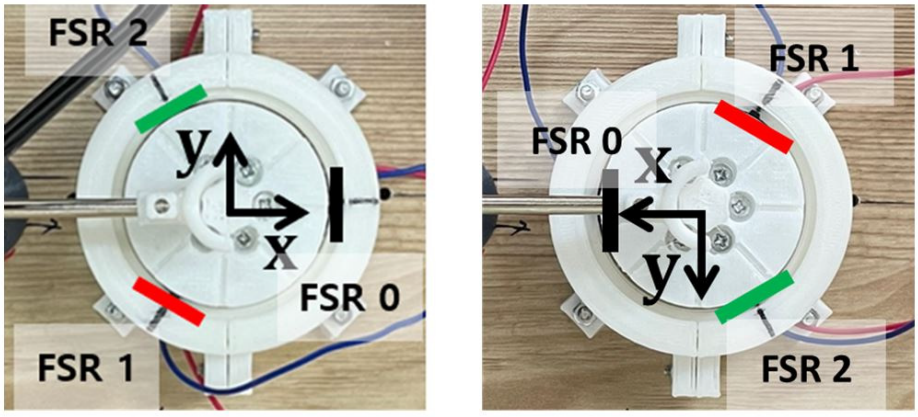

Figure 5. Axis configuration in (left) +x, and (right) -x direction

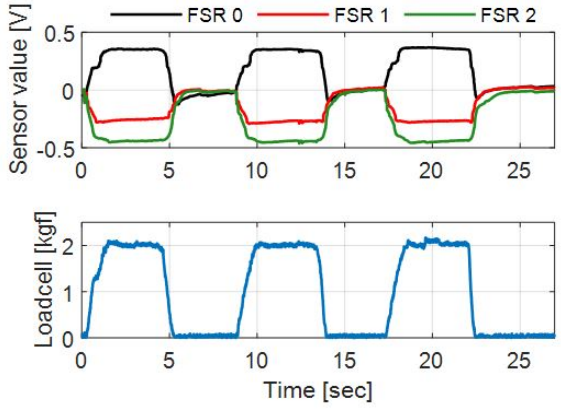

Figure 6. Experimental results of +x directional force

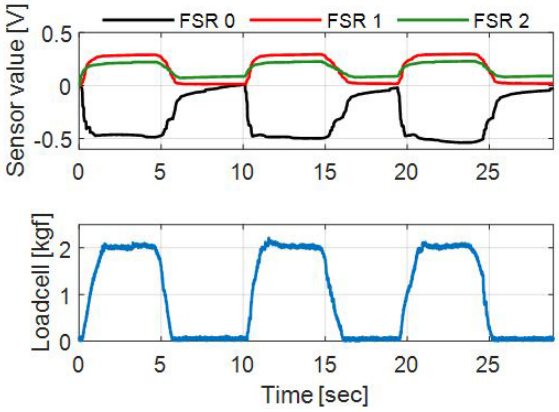

Figure 7. Experimental results of -x directional force

the same. The experimental results for the -x direction show FSR0 with negative values while FSR1 and FSR2 have similar positive values.

3.2.2. Y-axis pressure experiment

The experiment was conducted following the same method as the x-axis pressure experiment by applying forces ranging from 0 to 2 kg in both the +y and -y directions. **Figure 8** shows the experimental setup for applying forces in the +y and -y directions. In the case of y-axis force, as shown in **Figure 8**, FSR0 is oriented perpendicular to the y-axis, ideally resulting in no changes in its value. On the other hand, FSR1 and FSR2 are positioned at the same angle as the y-axis but in opposite directions, so they should yield measurement values with the same magnitude and opposite sign. **Figures 9** and **10** present the results of the experiment.

3.3. Derivation of bi-axial force relationships

The relationship between the measured force in each axis direction and the three FSR sensors obtained through experiments can be represented as shown in **Figure 11**. Due to the placement of FSR sensors spaced 120° apart, for x-axis force, FSR0 has a positive correlation, while FSR1 and FSR2 have similar magnitude negative correlations. For the y-axis force, FSR0 is minimally affected, FSR1 has a negative correlation, and FSR2 has a positive correlation. These relationships can be expressed as forces SF_x and SF_y calculated from the three sensor values.

$$\begin{bmatrix} SF_x \\ SF_y \end{bmatrix} = K \begin{bmatrix} FSR_0 \\ FSR_1 \\ FSR_2 \end{bmatrix} = \begin{bmatrix} k_{x0} k_{x1} k_{x1} \\ 0 k_{y1} - k_{y1} \end{bmatrix} \begin{bmatrix} FSR_0 \\ FSR_1 \\ FSR_2 \end{bmatrix} \quad (2)$$

To experimentally determine the value of that satisfies the above equation, the least mean squares method was used. The values obtained under the given

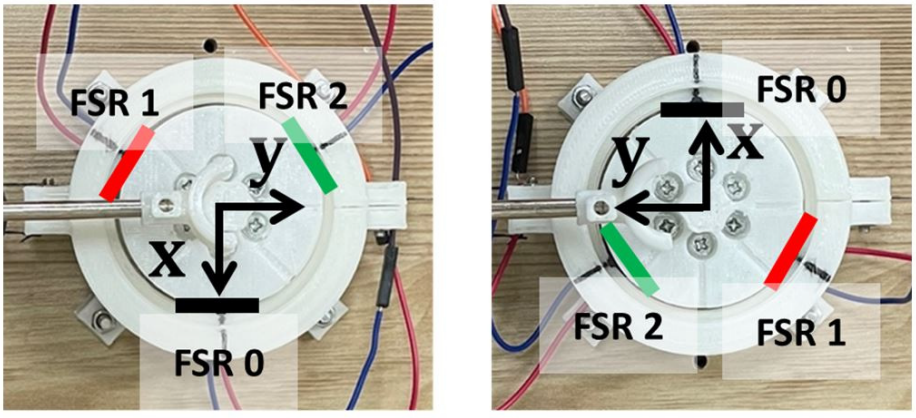

Figure 8. Axis configuration in (left) +y, and (right) -y direction

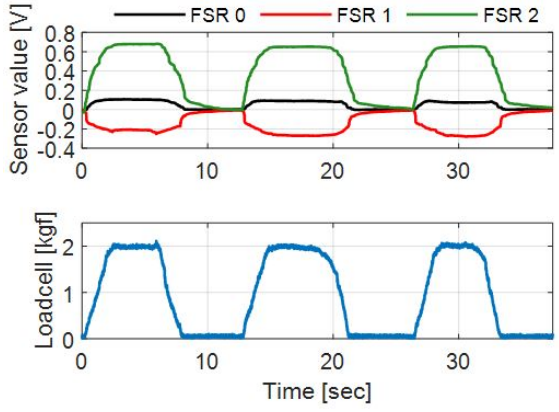

Figure 9. Experimental results of +y directional force

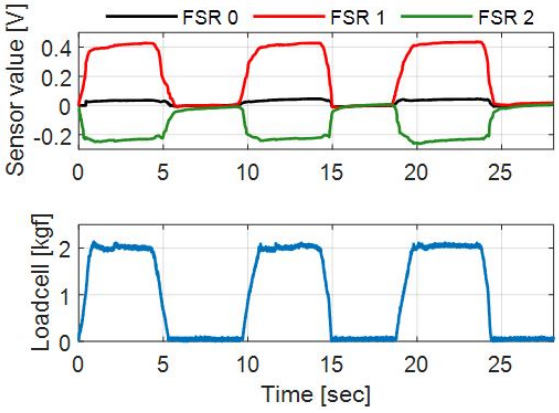

Figure 10. Experimental results of -y directional force

conditions are as follows.

$$K = \begin{bmatrix} 1.8287 & -1.7894 & -1.7894 \\ 0 & -2.2324 & 2.2424 \end{bmatrix} \quad (3)$$

Figure 12 shows the calculated forces SF_x and SF_y applying the derived value of . Positive correlation sensor forces with both x-axis and y-axis forces were obtained. However, the derived force measurements exhibit nonlinearity, which is characteristic of FSR sensors. To reduce the nonlinearity of sensor force values for each axis direction, they were approximated using a third-degree polynomial with load cell-measured force values.

$$F_x = a_1(SF_x)^3 + a_2(SF_x)^2 + a_3(SF_x) + a_4;$$
$$F_y = b_1(SF_y)^3 + b_2(SF_y)^2 + b_3(SF_y) + b_4 \quad (4)$$

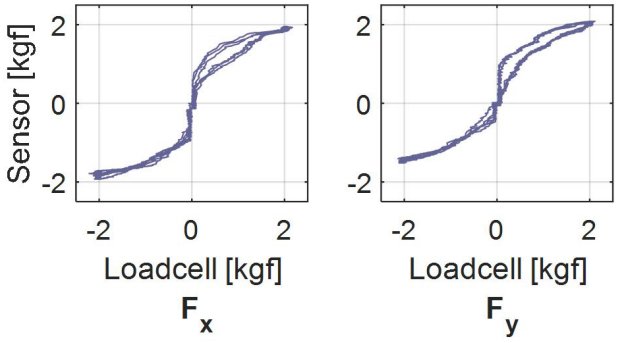

Figure 12. Relationship between x and y directional force and force calculated by sensor measurements

Using MATLAB's curve fitting toolbox, a_i and b_i were determined, and the results are summarized in **Table 1**.

The applied approximations for each axis direction's force measurements using the proposed sensor show a linear relationship with load cell measurements, as seen in **Figure 13**. **Figure 14** presents the time graphs of the x-axis force experiment and the y-axis force experiment. The R^2 values of the approximations were 0.9903 for F_x and 0.9928 for F_y.

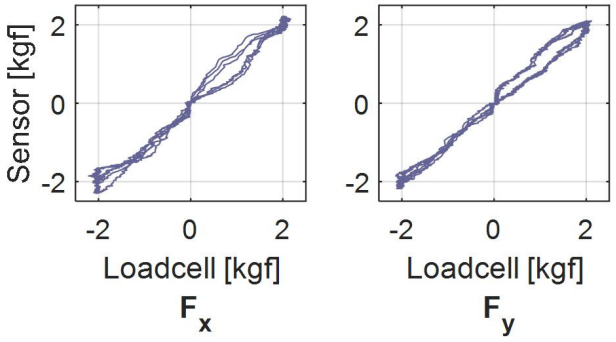

Figure 13. Calibrated force measurements

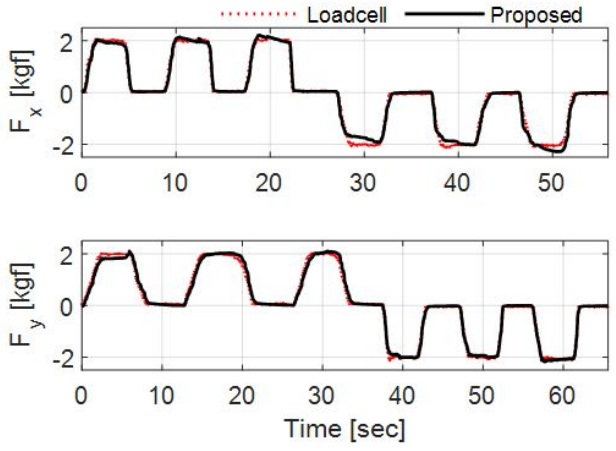

Figure 14. Force measurement results of the proposed sensor in the x and y direction

The accuracy of each axis direction's force was calculated using the following equation [17].

$$\%E_{i,acc} = \frac{\sum_{k=1}^{N} |F_i(k) - F_{i,loadcell}(k)|}{N \max |F_{i,loadcell}(k)|} \times 100 \quad (5)$$

Here, i=x, y and N is the total number of data samples. The calculated accuracy was 4.24% on the x-axis and 4.47% on the y-axis. The nonlinearity of

Table 1. Coefficients of fitting function

i	1	2	3	4
a_i	0.2722	-0.0322	0.1369	0.0405
b_i	0.2790	-0.2748	0.3685	-0.0081

each axis direction's force was calculated using the following equation (6).

$$\%E_{i,nlin} = \frac{\max\left|F_i(k) - F_{i,loadcell}(k)\right|}{F_{i,FSO}} \quad (6)$$

The calculated values were 11.17% for the x-axis and 9.37% for the y-axis.

3.4. Experiment with a wearable bi-axial force measurement device

The proposed bi-axial force measurement sensor module can be applied to various applications. It can be attached to the end effector of a robotic gripper or manipulator to measure multi-axis forces. To verify its potential utility before designing a multi-degree-of-freedom gripper, a simple wearable device was created as shown in **Figure 15(a)**. The bi-axial sensor module was worn on the palm using straps, and experiments were conducted by lifting a plastic box containing weights. The experiments involved lifting the box with both hands, as shown in **Figures 15(b)** and **15(c)**. The head wearing the sensor module was used without using fingers to lift the box; instead, the protruding head of the sensor was used to lift the box.

Figures 15(b) and **16(a)** depict the scenario of lifting the box in the +x direction and the corresponding measurement results. The initial state of the experiment began with the box placed on the floor. When lifting the box from the floor, it was held for 5 seconds and then placed back on the floor for another 5 seconds. This process was repeated twice, with an increment of 1 kg each time, up to a maximum of 2 kg. Due to the weight of the box, a -x direction force acted on the sensor, and the measurement results show that remains almost unchanged while increased with increasing weight. **Figures 15(c)** and **16(b)** depict the scenario of lifting the box in the +y direction and the corresponding measurement results. The sensor experienced a -y direction force due to the weight of the box, and as the weight increased, increased accordingly.

4. Conclusion

In this study, a bi-axial pressure sensor that can be installed on the end effector of a manipulator was fabricated. The proposed bi-axial pressure sensor was created using 3D printing for three components

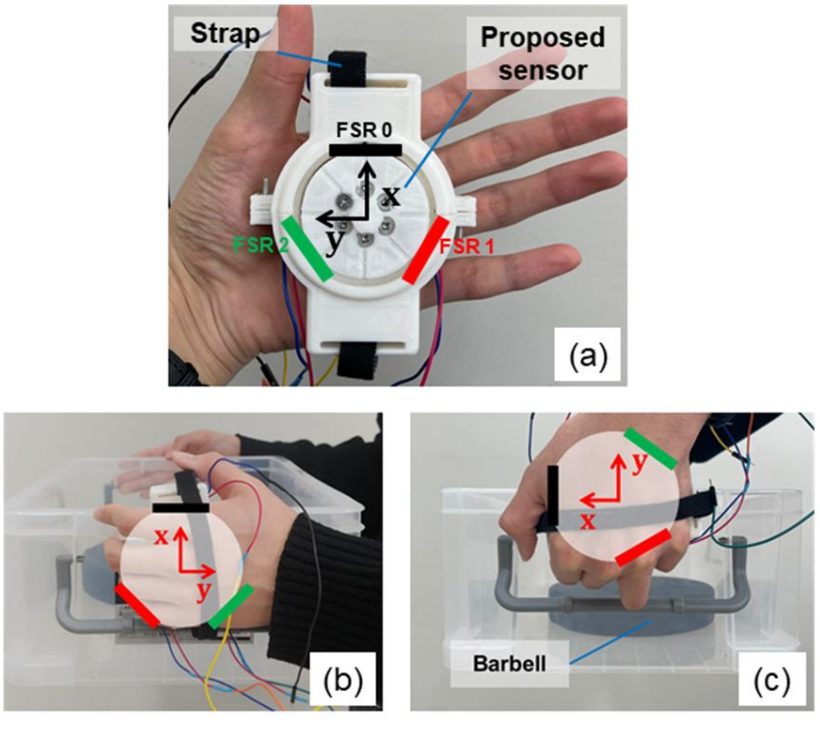

Figure 15. (a) Wearable device with a proposed sensor. Lifting a box in (b) the +x direction and (c) the +y direction.

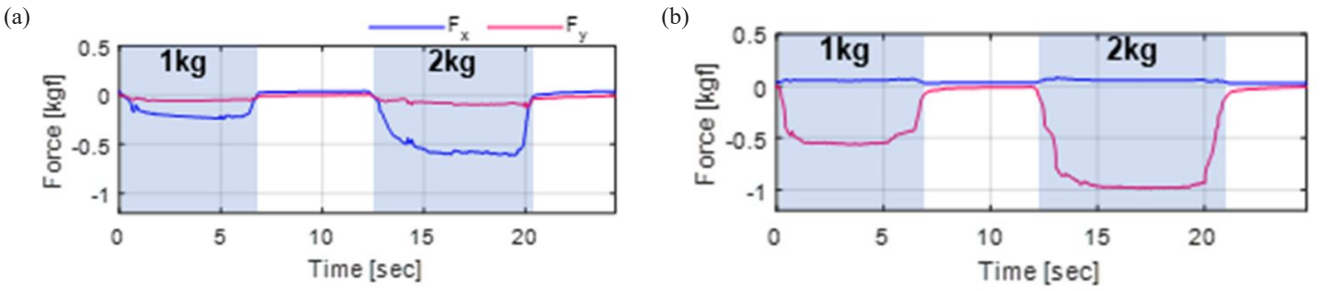

Figure 16. Box lifting results of (a) +x direction and (b) +y direction

and three commercial FSR sensors. PLA and TPU filaments, readily available in the market, were used, and the total cost for one sensor module, including the filaments used for printing and the FSR sensors, was approximately 20,000 KRW. Since it is designed as an assembly type, it has the advantage of easy replacement and reassembly in case specific components are damaged or FSR sensors reach the end of their lifespan.

The bi-axial force sensor features three FSR sensors arranged at 120° intervals and the design of the head component applies a certain initial pressure upon assembly. Due to these features, the compressive force applied to the FSR sensors varies relatively in both positive and negative values depending on the direction of the external force. After the fabrication, experiments were conducted using a load cell to apply a maximum force of 2 kg in the +x, -x, +y, and -y-axis directions. By observing the shape of the graphs according to the direction of the force, the correlation between each FSR sensor and the force direction was determined, and equations for deriving bi-axial force values from sensor values were established. The proposed sensor exhibited an accuracy of 4.24% and 4.47% for the x-axis and y-axis forces, respectively. Hysteresis occurred due to the non-linear characteristics of the FSR sensors and the elasticity of the TPU material, leading to nonlinearity in force measurements. Additionally, due to the limitations of the experimental setup, it was challenging to precisely control the direction of the applied force.

In the future, a force measurement method considering the nonlinearity of FSR sensors and elastic materials will be developed, and the performance of force measurement for cases where the force direction changes in real-time will be analyzed using commercial multi-axis sensors instead of uniaxial load cells. If a three-axis sensor capable of measuring z-axis force is produced, it is expected that it can be applied to various manipulator end-effectors.

Disclosure statement

The authors declare no conflict of interest.

Funding

This work was funded by the National Research Foundation (NRF) of Korea grant funded by the Korea government (MSIT) (No. 2021R1F1A1062499).

References

[1] Grosu V, Grosu S, Vanderborght B, et al., 2017, Multi-Axis Force Sensor for Human-Robot Interaction Sensing in a Rehabilitation Robotic Device. Sensors, 17(1): 1294. https://doi.org/10.3390/s17061294

[2] Jeong Y-S, Lee C-S, 2018, External Force Estimation by Modifying RLS using Joint Torque Sensor for Peg-in-Hole Assembly Operation. The Journal of Korea Robotics Society, 13(1): 55–62. https://doi.org/10.7746/jkros.2018.13.1.055

[3] Kim H-S, Kim G-S, 2017, Development of Calf Link Force Sensors of Walking Assist Robot for Leg Patients. Journal of Sensor Science and Technology, 26(2): 114–121. https://doi.org/10.5369/JSST.2017.26.2.114

[4] Wu B, Luo J, Shen F, et al., 2011, Optimum Design Method of Multi-Axis Force Sensor Integrated in Humanoid Robot Foot System. Measurement, 44(9): 1651–1660. https://doi.org/10.1016/j.measurement.2011.06.013

[5] Lee K-J, Kim H-M, Kim G-S, 2016, Design of Smart Three-Axis Force Sensor. Journal of Institute of Control, Robotics and Systems, 22(3): 226–232. https://doi.org/10.5369/JSST.2016.25.2.110

[6] Wasserfall F, Hendrich N, Fiedler F, et al., 2017, 3D-Printed Low-Cost Modular Force Sensors. Human-Centric Robotics: 485–492. https://doi.org/10.1142/9789813231047_0059

[7] Hendrich N, Wasserfall F, Zhang J, 2020, 3D Printed Low-Cost Force Torque Sensors. IEEE Access, 8: 140569–140585. https://doi.org/10.1109/ACCESS.2020.3007565

[8] Kim K, Park J, Suh J-H, et al., 2017, 3D Printing of Multiaxial Force Sensors Using Carbon Nanotube (CNT)/Thermoplastic Polyurethane (TPU) Filaments. Sensors and Actuators A Physical, 263: 493–500. https://doi.org/10.1016/j.sna.2017.07.020

[9] Mayetin U, Kucuk S, 2021, A Low Cost 3-DOF Force Sensing Unit Design for Wrist Rehabilitation Robots. Mechatronics, 78: 102623. https://doi.org/10.1016/j.mechatronics.2021.102623

[10] Chathuranga DS, Wang Z, Noh Y, et al. IROS 2016 – IEEE/RSJ International Conference on Intelligent Robots and Systems, October 9–14, 2016: A Soft Three Axis Force Sensor Useful for Robot Grippers. 2016, Daejeon. https://doi.org/10.1109/IROS.2016.7759817

[11] Viry L, Levi A, Totaro M, et al., 2014, Flexible Three-Axial Force Sensor for Soft and Highly Sensitive Artificial Touch. Advanced Materials, 26(17): 2659–2664. https://doi.org/10.1002/adma.201305064

[12] Kim S-J, Choi J-Y, Moon H-P, et al., 2016, Development of Polymer Slip Tactile Sensor Using Relative Displacement of Separation Layer. The Journal of Korea Robotics Society, 11(2): 100–107. https://doi.org/10.7746/jkros.2016.11.2.100

[13] Song K, 2020, HASEL Actuator Study for Tactile Feedback Device. The Journal of Korea Robotics Society, 16(1): 12–16. https://doi.org/10.7746/jkros.2021.16.1.012

[14] Vogt DM, Park Y-L, Wood RJ, 2013, Design and Characterization of a Soft Multi-Axis Force Sensor Using Embedded Microfluidic Channels. IEEE Sensors Journal, 13(10). https://doi.org/10.1109/JSEN.2013.2272320

[15] Kim K, Ahn J, Jeong Y, et al., 2021, All-Soft Multiaxial Force Sensor Based on Liquid Metal for Electronic Skin. Micro and Nano Syst Lett, 9(2). https://doi.org/10.1186/s40486-020-00126-9

[16] Y Mengüç, Park Y-L, Pei H, et al., 2014, Wearable Soft Sensing Suit For Human Gait Measurement. The International Journal of Robotics Research, 33(14). https://doi.org/10.1177/0278364914543793

[17] Choi H, Kong K, 2019, A Soft Three-Axis Force Sensor Based on Radially Symmetric Pneumatic Chambers. IEEE Sensors Journal, 19(13). https://doi.org/10.1109/JSEN.2019.2904606.